11

ENSO and Tropical Cyclone Activity

Pao-Shin Chu

The present state of knowledge regarding tropical cyclone activity in various ocean basins and the El Niño–Southern Oscillation phenomenon is reviewed in this chapter. The ocean basins include the western North Pacific, the eastern and central North Pacific, the southwestern Pacific, the southeastern Pacific, and the North Atlantic. Following a description of the ENSO phenomenon, tropical cyclone activity in each basin is discussed in the context of frequency, genesis location, track, life span, and intensity.

For the western North Pacific, the pronounced change in tropical cyclone activity due to warm ENSO is the eastward and equatorial shift in genesis location, longer life span, and more recurvature of tropical cyclone tracks (Chan, chapter 10 in this volume). There is also a notable decrease in tropical cyclone counts in the year following a warm ENSO event. For the eastern North Pacific, the formation point shifts farther west, more intense hurricanes are observed, and tropical cyclones track farther westward and maintain a longer lifetime in association with warm ENSO events. The central North Pacific sees more tropical cyclone counts in the El Niño year due to more tropical cyclone formation in this region and a tendency for tropical cyclones that originate in the eastern North Pacific to enter the central North Pacific. As in the North Pacific, tropical cyclones in the South Pacific originate farther east during El Niño years, resulting in more storms in the southeastern Pacific and fewer storms in the southwestern Pacific. The North Atlantic features fewer tropical cyclone counts, slightly weaker intense storms, and hurricane genesis farther north during El Niño years. Changes are approximately opposite in cold ENSO years.

Interest in the relationship between tropical cyclone activity in various ocean basins and the El Niño–Southern Oscillation (ENSO) phenomenon has grown over the last two decades. This interest is drawn from the fact that large-

scale environmental conditions conducive to tropical cyclone activity (e.g., formation, track, frequency, life span, landfall, and/or intensity) during El Niño years differ profoundly from those of climatological or La Niña years. The El Niño phenomenon is manifested in the anomalous warming of the eastern and central tropical Pacific. La Niña refers to anomalous cooling of the tropical Pacific, or simply the opposite of El Niño. Because ENSO, as first recognized by Bjerknes (1969), is a powerful interplay between the tropical ocean and atmosphere in the Pacific Basin and because tropical cyclones form mainly in the tropics, modulation of tropical cyclone activity by ENSO is expected.

There is an extensive body of literature relating seasonal tropical cyclone activity in various ocean basins to ENSO. Gray (1984) and Gray and Sheaffer (1991) ascribed Atlantic seasonal hurricane frequency to El Niño and the Quasi-Biennial Oscillation of stratospheric wind. Through statistical analyses, Shapiro (1987) and Goldenberg and Shapiro (1996) further confirmed the dependence of tropical cyclone formation in the Atlantic on ENSO. For the western and eastern North Pacific, Chan (1985, 2000), Lander (1994), Chen et al. (1998), and Irwin and Davis (1999) noted a shift in tropical cyclone genesis location during El Niño and La Niña phases. Chu and Wang (1997), using actual tropical cyclone observations and statistical resampling techniques, found more tropical cyclone occurrences in the vicinity of Hawai'i in the central North Pacific when El Niño occurred as compared to non–El Niño years. Tropical cyclone activity in the South Pacific is likewise influenced by ENSO (e.g., Nicholls 1979, 1985; Sadler 1983; Revell and Goutler 1986; Hastings 1990; Basher and Zheng 1995; McBride 1995). More recently, Landsea (2000) reviewed the relationship between tropical cyclone activity and ENSO but focused on the Atlantic Ocean. In particular, he addressed the issue of seasonal predictability of tropical cyclones over the Atlantic Ocean.

This chapter first describes the ENSO phenomenon before discussing tropical cyclone activity in several ocean basins in relation to ENSO. The ocean basins include the western North Pacific and the South China Sea, the eastern and central North Pacific, the South Pacific, and the North Atlantic (figure 11.1). Because the ENSO signal in the Indian Ocean is weak, ENSO influences on tropical cyclone activity in the North and South Indian Oceans are not considered in this chapter but further investigations may discover significant correlations (but see Jury 1993).

General Descriptions of ENSO

Originally, the name El Niño (Spanish for the Christ child) was given to a weak coastal current that flows southward along the coast of Ecuador and Peru

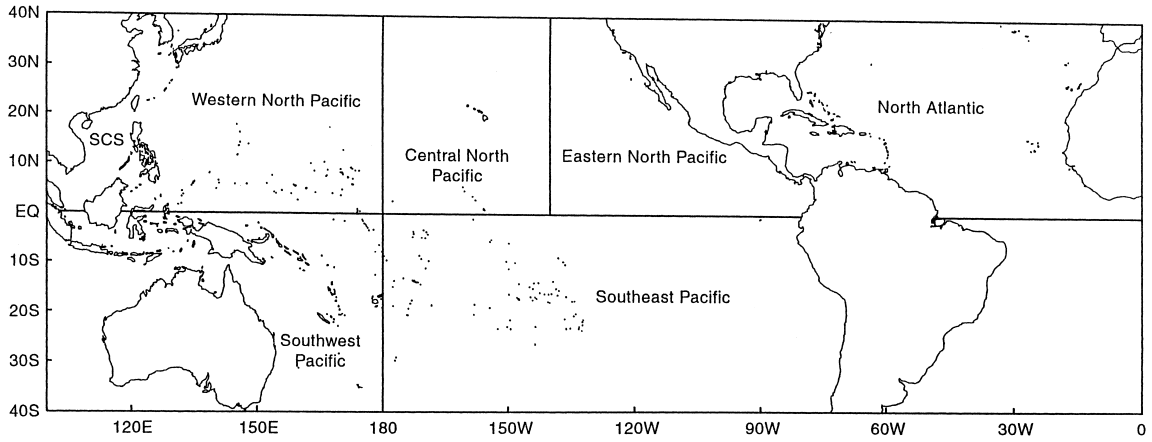

FIGURE 11.1 Orientation map of the western North Pacific and the South China Sea (denoted as the SCS), the eastern and central North Pacific, the southwestern Pacific, the southeastern Pacific, and the North Atlantic Basin.

around Christmastime. This occurs during the austral summer, when local winds are weak and the upwelling of cold waters that carry the primary food source for fish is reduced (Bjerknes 1969; Wyrtki 1975). As a result, the ocean surface along the west coast of tropical South America becomes anomalously warm. In some years the upwelling terminates abruptly, the ocean surface warms extensively, and fish starve from the lack of foods nourished by the nutrient-rich, upwelled cold water. These conditions are disastrous for the fishery industry and local economy in Ecuador and Peru.

In broad terms, the La Niña (Spanish for "the girl") phenomenon can be regarded as the opposite of the El Niño condition. During La Niña, easterly trade winds are strong and persistent, blowing from a region of high pressure over the southeastern Pacific toward a region of low pressure in the western Pacific where warm pools of water with light winds and convection prevail (e.g., Deser and Wallace 1990). Because surface winds in the tropics mainly follow the pressure gradient, easterly winds prevail. The easterly winds not only induce equatorial Ekman upwelling because of the Coriolis effect, creating a cold tongue in the equatorial eastern to central Pacific, but they also raise sea level in the west and lower it in the east. Thus, a west-east sea level slope occurs across the Pacific (figure 11.2a). The thermocline, an interface separating warm and relatively low-density water in the upper ocean from cold, high-density water in deep ocean, is relatively deep in the western Pacific (~ 220 m) but shallow off the west coast of South America (~30 m). The zonal difference in thermocline depth results in equatorial ocean dynamics that play a key role in ENSO perturbations (Cane and Zebiak 1985).

In the atmosphere, a zonal circulation along the equatorial Pacific occurs with rising air over the warm Indonesian region and sinking air over the cold eastern Pacific. The vertical air movement is connected by easterlies in the lower troposphere and westerlies in the upper troposphere. The zonal sea surface temperature gradient with cold water in the east and warm water in the west is considered the cause of this thermally driven direct circulation. Bjerknes (1969) named this circulation cell the Walker circulation. There is a positive feedback between the atmosphere and ocean in the tropics because surface winds drive ocean currents, and these currents redistribute surface thermal gradients that affect wind fields through hydrostatic effects in surface pressures.

The pioneering work by Bjerknes (1969) and Wyrtki (1975) laid the foundation for numerous theoretical and modeling studies pertinent to the ENSO phenomenon (e.g., McCreary 1983; Zebiak and Cane 1987). In a dynamical framework, the fundamental roles in the development of El Niño are played by oceanic Kelvin waves in the equatorial waveguide, off-equatorial Rossby waves, and reflections by the western boundary of the tropical Pacific (Schopf and

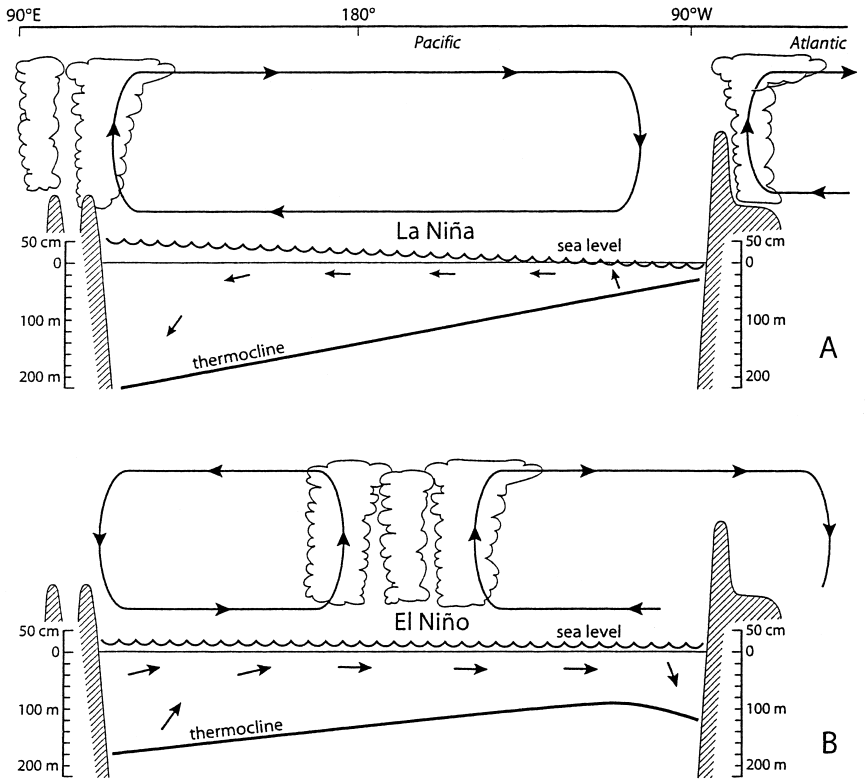

FIGURE 11.2 Schematics showing the near-equatorial atmosphere and ocean circulations in the Pacific and western Atlantic associated with the (*A*) La Niña and (*B*) El Niño conditions. During El Niño, major convection shifts eastward to the central Pacific, with subsidence over the western Pacific and the western Atlantic. During El Niño, oceanic currents flow eastward, the thermocline deepens along the South American coast, and sea level drops and the thermocline rises in the western Pacific (adapted from Wyrtki 1982).

Suarez 1988; Battisti and Hirst 1989). These phenomena interact and produce changes in sea-surface temperatures, the thermocline, and sea level. Note that Kelvin waves are equatorially trapped waves that propagate rapidly eastward. In contrast, Rossby waves propagate to the west relative to the zonal mean flow.

Wyrtki (1975) recognized from an analysis of observations that prior to an El Niño event there is a buildup of warm water between sea level and the thermocline in the western Pacific warm pool. As soon as easterly trade winds relax, the accumulated warm water flows eastward in the form of Kelvin waves to give rise to an El Niño event. The oceanic Kelvin waves, excited by episodic westerly wind bursts in the western and central Pacific, propagate rapidly eastward across the equatorial Pacific in a period of two to three months. These waves

are responsible for the deepening of the thermocline in the eastern Pacific (figure 11.2b). Consequently, cold water from below cannot be upwelled efficiently and the normal steep slope of the transbasin thermocline levels off (e.g., Lukas, Hayes, and Wyrtki 1984). The eastward advection of warm water caused by changes in the zonal component of the surface winds in the western Pacific that trail the Kelvin waves, and a deepened thermocline induced by downwelling Kelvin waves cause sea-surface temperatures in the equatorial central to eastern Pacific to become anomalously warm. The wind anomalies also generate westward propagating Rossby waves in the off-equatorial Pacific that reflect at the western boundary and return as delayed Kelvin waves. In analyzing daily wind observations for a 30-year period, Chu, Frederick, and Nash (1991) noted an increased frequency of westerlies in the equatorial western Pacific during an El Niño period.

At the height of El Niño events, warm pools of seawater, low-level westerlies, and the attendant tropical convection shift from the western Pacific to the central or eastern Pacific (figure 11.2b). Accordingly, the rising branch of the Walker circulation is located in the equatorial central Pacific and the sinking branch is found over the western Pacific. Note that anomalies of large-scale flows are implied. As will be described later, these changes in atmospheric and oceanic circulation patterns during El Niño have profound impacts on regional tropical cyclone activity. The monsoon trough is regarded as the breeding ground of tropical cyclones and normally occurs near large land masses in the western Pacific where the monsoonal effects are pronounced. This trough is marked by a low-level wind shear line, with monsoon westerlies on its equatorward side and easterly trade winds on its poleward side. During an El Niño the monsoon trough is displaced to the east (Lander 1994; Clark and Chu 2002).

Barnston, Chelliah, and Goldenberg (1997) determined that the El Niño phenomenon is most reliably reflected in the equatorial sea-surface temperature from approximately 120ºW westward to near the date line. As a result, one of the most popular indices used to monitor El Niño is the areally averaged sea-surface temperature in the Niño 3.4 region. The Niño 3.4 region covers an area between 5ºN to 5ºS and 170ºW to 120ºW and is close to the Pacific warm pool and the major center of convection during El Niño (figure 11.2b). Trenberth (1997) defined El Niño and La Niña events on the basis of the 5-month running mean of sea-surface temperature anomalies in the Niño 3.4 region exceeding positive and negative 0.4ºC, respectively, for at least 6 consecutive months. Using this definition, El Niño events have been as short as 7 months (1951–1952) and as long as 19 months (1986–1988). Since 1950, on average, an event starts in May or June and ends in the following April. The average length of an event is about 11.8 months, or almost one year. For La Niña, the

start and end months are similar to El Niño, but the average duration is 13.3 months, a little longer than El Niño. Furthermore, a neutral state of Pacific sea-surface temperatures occurs 45% of the time when El Niño or La Niña conditions are absent (Trenberth 1997).

Each El Niño has its own characteristic onset and demise time, duration, magnitude, exact place of maximum warming, phase propagation, and so on. Although each episode behaves differently, there is a tendency for the maximum amplitude of major events to occur near the end of the calendar year so it is phase-locked to the annual cycle. The El Niño and La Niña phases are also known to change preferentially around March-April when surface winds are weak, sea-surface temperatures in the equatorial cold tongue are warm, and the east-west sea-surface temperature gradient along the equatorial Pacific is slack (e.g., Lee et al. 1998). This is the time when atmosphere and ocean coupling is weakest. Prior to an El Niño, relatively large amounts of anomalously warm water accumulates between the sea level and the thermocline in the western Pacific warm pool (Wyrtki 1975, 1985). The excess heat content in this warm water is then discharged toward off-equatorial regions and into the atmosphere during El Niño. It has been suggested that the discharge and recharge of heat contained in the equatorial water is the key ingredient that controls the transition between El Niño and La Niña phases (Wyrtki 1975, 1985; Cane and Zebiak 1985; Jin 1997).

Changes in atmospheric pressure patterns between centers in the Pacific and Indian oceans are associated with changes in sea-surface temperatures and oceanic heat contents during El Niño. As pressures fall in the eastern South Pacific subtropical high, they tend to rise in the Indonesian low-pressure zone. The term "Southern Oscillation" (SO) was coined to describe the zonal, atmospheric mass exchanges across two southern oceans. To monitor the behavior of such a large-scale atmospheric circulation, the Southern Oscillation Index (SOI) is used. The standard SOI used by many operational weather and climate agencies and researchers throughout the world is derived from a difference in normalized sea level pressures between Tahiti and Darwin, Australia. Because the Southern Oscillation is closely linked with El Niño, both events are labeled collectively ENSO. Although not periodic, the ENSO phenomenon generally recurs every three to four years, but the time between past events has ranged between two and seven years (Trenberth 1976). Using a time-domain approach, Chu and Katz (1989) independently found a dominant spectral peak between three and four years in the SOI series.

Because ENSO has an immense impact on tropical cyclone activity, real-time ENSO forecasting has been performed by numerous researchers, institutes, and national meteorological centers around the world. In general,

dynamical or statistical models are used in the forecasting enterprise, and these forecast results have been published routinely in the Experimental Long-Lead Forecast Bulletin (e.g., Kirtman 2001). For dynamical models, the degree of complexity varies from simple, linear shallow-water equations for both ocean and atmosphere, to intermediate coupled ocean-atmosphere models, to hybrid coupled models (e.g., statistical atmosphere and comprehensive ocean circulation), to fully coupled ocean-atmosphere models with multiple vertical layers. In comparison to dynamical models, statistical models are more simple and use less computer time and storage space.

By considering the persistence of initial conditions, trend, and climatology of past ENSO events, Knaff and Landsea (1997) developed a multiple regression model to forecast Niño 3 and Niño 3.4 region sea-surface temperature anomalies. They called it an ENSO-CLIPER model. The idea of the ENSO-CLIPER model is derived from the tropical cyclone community in which a simple CLIPER (i.e., Climatology plus Persistence) scheme has long been used as a benchmark against other more sophisticated models for storm-track prediction (e.g., Neumann 1977). Landsea and Knaff (2000) compared forecast skills of their ENSO-CLIPER baseline system with other dynamical and statistical models for the very strong 1997–1998 El Niño event. They noted that at short lead time (up to eight months ahead), the ENSO-CLIPER has the smallest root-mean square error among all models tested. This result is rather intriguing because forecasts made by the ENSO-CLIPER are considered as having no-skill. If forecasts for the 1997–1998 ENSO event are representative of other cases, then there is very little or no skill in ENSO prediction, despite the great efforts to develop sophisticated numerical models.

Throughout this chapter, the terms "El Niño," "warm ENSO phase," and "warm phase" are used interchangeably. Likewise, the terms "La Niña," "cold ENSO phase," and "cold phase" are used interchangeably. The term "neutral phase" describes conditions when sea-surface temperatures are near climatological averages. Note that a large and negative SOI lasting several months generally corresponds to a warm ENSO phase, and a large and positive SOI persisting several months is indicative of a cold phase. As a cautionary note, it should be mentioned that some abrupt changes occur occasionally in the monthly SOI (Chu and Katz 1985). For instance, the monthly SOI may fluctuate from a positive value in one month to a negative value in a second month, followed by a positive value in a third month, or vice versa. The Tropical Intraseasonal Oscillation (Madden and Julian 1971), which has a typical time scale of 30 to 50 days, may perturb the large-scale mass circulation in the SO regime on a short-term basis. As a result, the monthly SOI is occasionally contaminated by some transient circulation features (e.g., mid-latitude troughs and ridges during the austral winter)

that are not inherent in the large-scale SO. In this regard, sea-surface temperature in the equatorial Pacific may serve as a more robust indicator of the state of ENSO phase than the SOI because of the well-known slow change in thermal content and large heat capacity of tropical oceans.

The Western North Pacific

Climatologically, tropical cyclone frequency (i.e., tropical storms and typhoons) in the western North Pacific is higher than in any other ocean basin, with an annual mean value of 26, based on 22-year statistics from 1968 to 1989 (Neumann 1993). The standard deviation of annual tropical cyclone counts is 4.1. The western North Pacific is also the only basin where tropical cyclone formation is observed throughout the 12 months of the year, although a majority of cyclones develop between June and November (Frank 1987).

Studies by Chan (1985, 2000, chapter 10 in this volume), Dong (1988), Lander (1994), Chen et al. (1998), and Kimberlain (1999) establish a relationship between tropical cyclone activity in the western North Pacific and El Niño and La Niña phenomena. Through spectral and cross-spectral analyses, Chan (1985) found that both the SOI and typhoon count series possess a dominant peak in the frequency band of 3 to 3.5 years and that the SOI leads typhoon series by about one year in this band. That is, a large and negative SOI (i.e., a warm ENSO phase) tends to be followed by an overall reduction in tropical cyclone frequency over the western North Pacific in the following year, and vice versa. In addition, Chan (1985) and Dong (1988) noted that tropical cyclone genesis location shifts eastward across 150°E in the western Pacific during warm ENSO years (figure 11.1). Therefore, more typhoons and tropical storms occurred in the eastern part (150°E to the date line) than the western part of the western North Pacific (120°E–150°E) during an El Niño event.

Lander (1994), however, only found a weak correlation between annual tropical cyclone counts in the entire western North Pacific Basin and ENSO, but he concurred with Chan and Dong in terms of the eastward displacement of the genesis location during an El Niño and the westward retreat in the genesis location during La Niña. This zonal displacement is intimately related to the low-level monsoon trough where its mean over-water position in August stretches from southeast to northwest over the Philippine Sea and southern Taiwan (figure 11.3). The monsoon trough is marked by moist, southwest monsoon flows to the south and easterly trades to the north of the trough. Tropical disturbances are often found in the trough where there is a weak cyclonic rotation. As the cyclonic spin in the trough increases, these systems tend to inten-

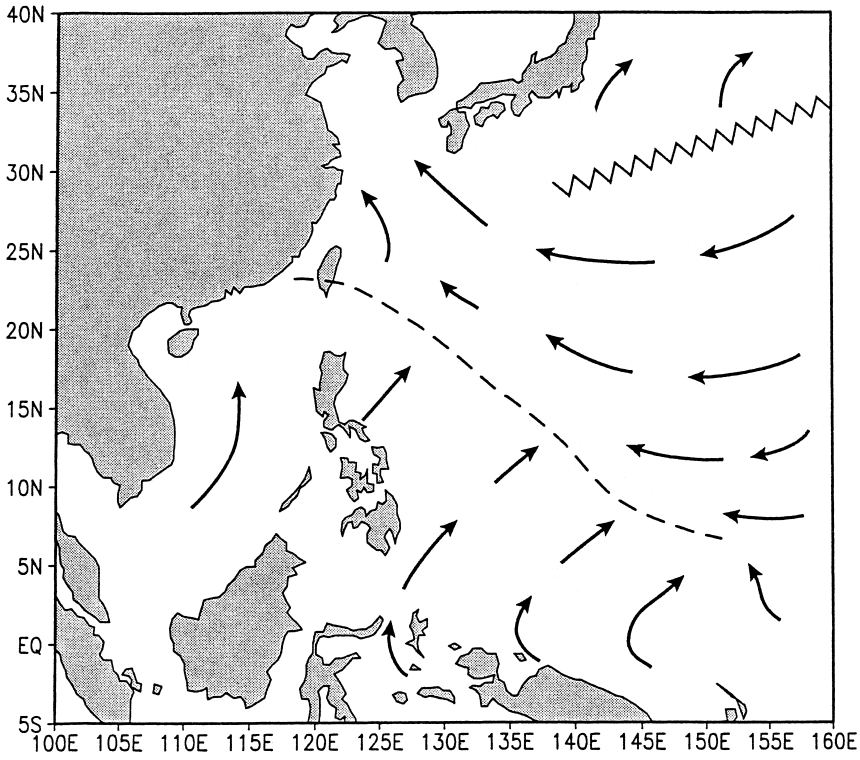

FIGURE 11.3 Schematic showing the long-term mean surface circulation in August in the western North Pacific. The monsoon trough axis is denoted as a broken line, and the ridge axis is denoted as a zigzag line. Wind directions are indicated by arrows.

sify into tropical storms or typhoons (Sadler 1967). It should be kept in mind that the position of the trough in figure 11.3 is only meant to represent the long-term mean condition. In any given summer month, this trough may deviate substantially from its mean position. For instance, at times the monsoon trough extends in an elongated east-west direction from the Philippine Sea to the date line, being reversed from its mean position (figure 11.3); or it is not identifiable at all (Lander 1996).

More recently, Chan (2000, chapter 10 in this volume) stratified tropical cyclone frequency month by month according to the ENSO cycle. During an El Niño year, tropical cyclone activity over the South China Sea is below normal in September and October but above normal in the eastern portion of western North Pacific. For the year immediately following an El Niño event, tropical cyclone formation is below normal over the entire western North Pacific Basin (Chan 2000). Conceivably, because of the eastward shift in the major

convection and the rising branch of the Pacific Walker cell during El Niño, the western North Pacific sees a compensating subsidence that would be unfavorable for tropical cyclone formation. The cooler ocean surfaces and higher sea level pressures in the western Pacific that characteristically occur during El Niño years (Rasmusson and Carpenter 1982; Deser and Wallace 1990) may also contribute to the reduction of tropical cyclone frequency. For the La Niña composite, tropical cyclone frequency over the western North Pacific and South China Sea varies inversely to that during El Niño years.

The trough and monsoon westerlies extend eastward, in some years beyond the date line during a warm ENSO event; therefore it is no surprise that the genesis location of tropical cyclones shifts eastward. This is seen in figure 11.4, which portrays the easternmost location of the trough in boreal summer and autumn for each year. The monsoon trough is displaced farther eastward in autumn than in summer, which is consistent with the results described by Lander (1994) and Chen et al. (1998). In the years 1972, 1982, 1994, and 1997, the autumn mean location of the monsoon trough extends eastward past the date line into the central North Pacific (figures 11.4 and 11.1).

To illustrate the influence of monsoon trough on tropical cyclone development, figure 11.5 shows the genesis location of tropical cyclones during the six

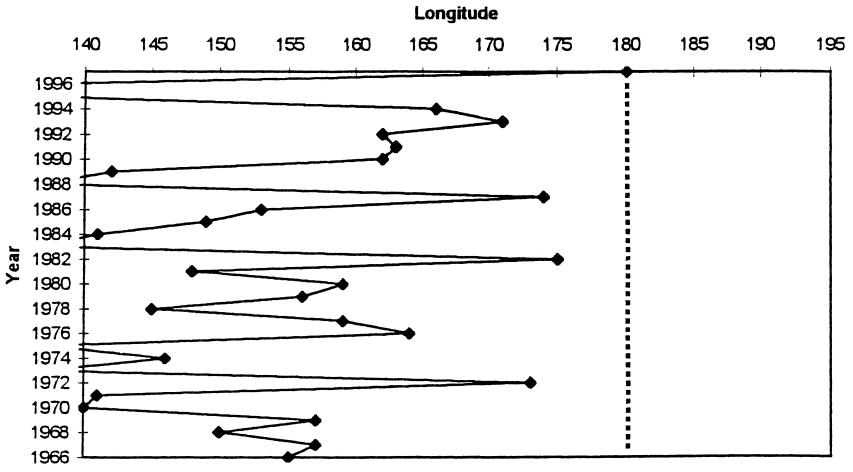

FIGURE 11.4 Time series of the farthest eastward extent of the monsoon trough at the 1,000 hPa level in the western and central North Pacific for the years 1966 to 1997 for (*a*) boreal summer (June-August) and (*b*) boreal autumn (September-November) means. The date line is indicated as a broken line. In (*b*), Ws denote six warmest ENSO years and Cs denote four out of six coldest ENSO years. Years refer to the period of June to November. The year 1994 was also a warm ENSO year, but the SST anomalies averaged during the typhoon season in that year do not qualify for the top six warmest years.

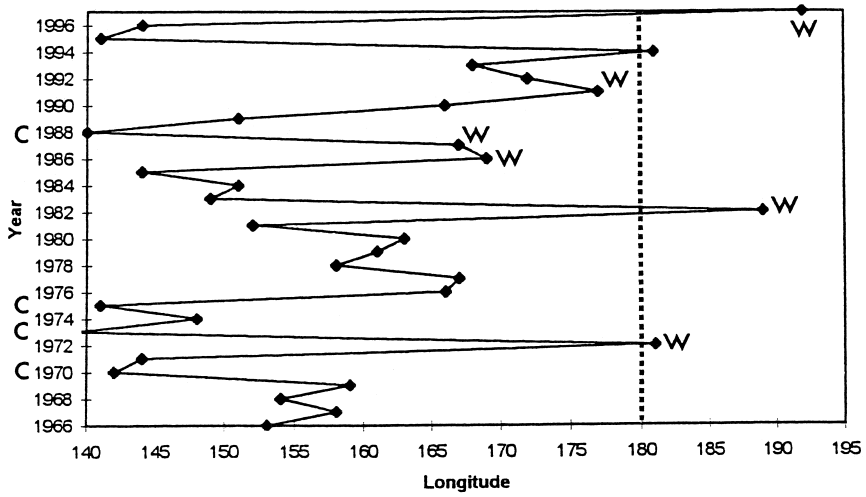

FIGURE 11.4 *(Continued)*

warmest and six coldest ENSO years using data from 1970 to 2000, a period when estimations of typhoon counts are thought to be more reliable (Kimberlain 2000). Here only tropical cyclones that reached at least tropical storm stage are considered. Typhoon season (June to November) means of the Nino 3.4 region sea-surface temperature anomalies were calculated and utilized to define extreme years. Out of the last 31 years, the six warmest ENSO years for which the mean sea-surface temperature during the typhoon season are highest include 1972, 1982, 1986, 1987, 1991, and 1997. The six coldest ENSO years, when the mean sea-surface temperatures during the typhoon season are lowest, are 1970, 1973, 1975, 1988, 1998, and 1999. The early season refers to April through June, peak season runs from July through October, and late season goes from November to December.

Relative to the La Niña samples, the eastward shift in genesis locations is more pronounced in early and late seasons during El Niño years (figure 11.5). For instance, in the early season, most formation points are in the Philippine Sea during the La Niña years, but during El Niño years one third of the formation points lies east of 150°E. In the late season, origin points during El Niño years can be found as far east as 170ºE to 175ºE in the Marshall Islands. For the La Niña composite, tropical cyclone origin points are confined to the west of 140ºE in early season and to the west of 150ºE in late season. There is also a tendency for tropical cyclones to form closer to the equator during El Niño years as compared to La Niña years, and this meridional shift is particularly clear in peak and late seasons. During La Niña years, tropical cyclone genesis

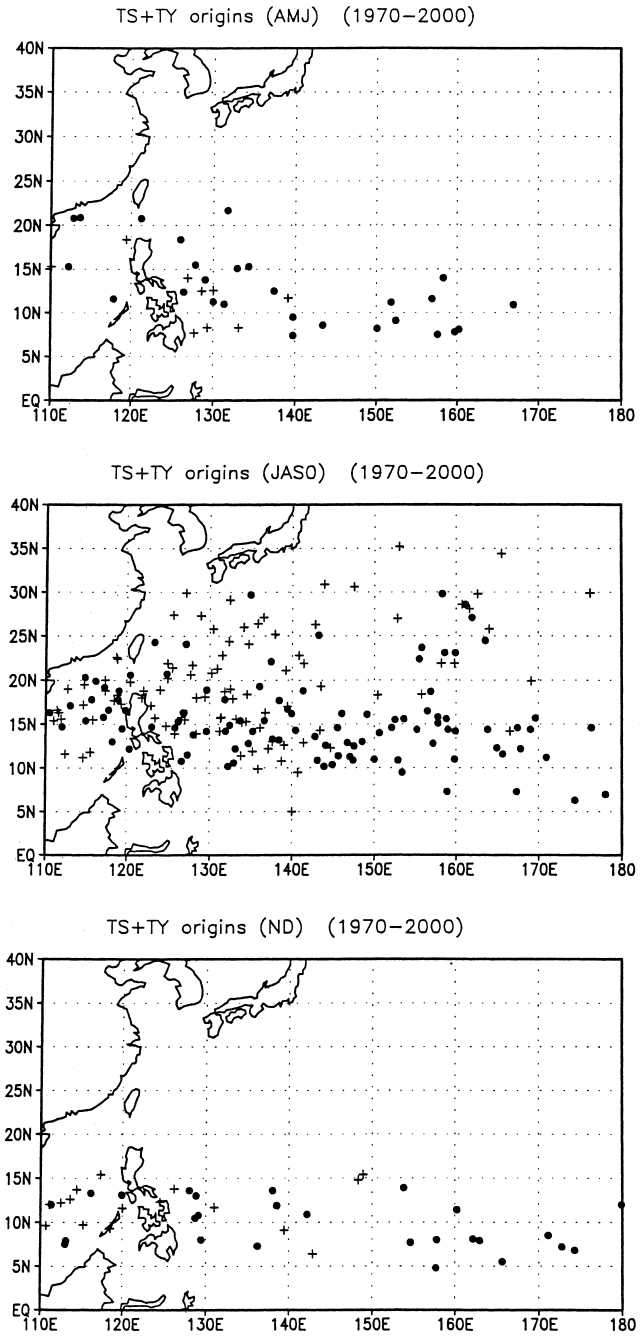

FIGURE 11.5 Origin points of tropical cyclones (tropical storms and typhoons) in the western North Pacific by season for six years during which the June through November mean sea-surface temperatures in the Niño 3.4 region are highest (represented by dots) and lowest (represented by crosses). Origin points refer to first tropical storm intensity location. The period used is 1970 to 2000. Early season refers to April to June (AMJ), peak season for July to October (JASO), and late season for November and December (ND).

locations in peak season stay at higher latitudes (20°N–30°N) over the western extreme of the North Pacific, being closer to the East Asian landmass. In the late season, most genesis points are found approximately equatorward of 15°N, regardless of warm or cold ENSO phases. In the South China Sea, more named storms formed in the early season of El Niño years but slightly more tropical cyclones formed in the late season during La Niña years.

An important environmental factor that modulates seasonal tropical cyclone activity is the vertical wind shear (Gray 1977). When tropical cyclones move into an area of strong vertical shear, the low-level center loses its upper level outflow channel and usually dissipates quickly (Gray 1968). Strong vertical shear also disrupts the organization of deep convection around the low-level center, which inhibits intensification of the incipient disturbance. Tropospheric vertical wind shear is hereafter defined as the magnitude of the difference between the zonal and meridional wind at 200 hPa and 850 hPa. Clark and Chu (2002) demonstrated a substantial reduction in vertical shear equatorward of 18°N over the eastern portion of the western North Pacific during an El Niño composite compared to the La Niña.

The eastward and equatorward shift in origin locations during El Niño years allow tropical cyclones to maintain a longer life span while tracking westward over open water. During La Niña years such as 1970, 1973, 1975, and 1988, when easterly winds prevailed in the western Pacific, the monsoon trough is short and confined in the western extreme of the North Pacific (figure 11.4). Accordingly, the genesis location is farther to the west and north. Being closer to the East Asia continent, cyclones that spawn along the monsoon trough are either on a collision course with land masses or being steered by a migrating upper-level trough away from the continent toward mid-latitude oceans. Once tropical cyclones move over a large land mass or over cold water, they lose intensity rapidly because the warm and moist air in a tropical cyclone is being cut off and the release of latent heat is greatly diminished. Furthermore, there is a substantial reduction in typhoon wind speeds over land because of increased surface roughness. Therefore, tropical cyclones during La Niña years will not be able to survive for as long as those mainly over lower latitude water during El Niño years. The number of named storm days and typhoon days in the western North Pacific Basin during El Niño years is nearly 1.5 times as large as that during La Niña years (Kimberlain 1999). Kimberlain (1999) applied a two-sample *t*-test and noted that the difference in tropical cyclone longevity between warm and cold ENSO years is statistically significant at the 5% level (a p-value of 0.01).

In addition to tropical cyclone frequency, genesis location, and longevity described previously, the tropical cyclone track in the western North Pacific

varies considerably between El Niño and La Niña years. During peak season, tropical cyclones tend to recurve during El Niño years but they track farther northward after being formed at higher latitudes during La Niña years (Kimberlain 1999; Wang and Chan 2001) (figure 11.5). During the El Niño summer, the mid-tropospheric western Pacific subtropical high shifts eastward and upper-level troughs tend to deepen along the east Asian coast (Wang and Chan 2002). Accordingly, tropical cyclones from the western Pacific are likely recurved by upper-level troughs. Furthermore, because tropical cyclones during El Niño years have longer life spans, they have a better chance to interact with transient midlatitude synoptic systems, resulting in more recurved trajectories. In the late season, tropical cyclones continue to recurve during El Niño years, but during La Niña years they tend to move westward around the southern flank of the elongated subtropical high toward the Philippines and the South China Sea. In assessing the relative importance of typhoon landfalls (not origin points) associated with two contrasting climatic events, Saunders et al. (2000) found that typhoon impacts in Japan, South Korea, Taiwan, and China are more pronounced during El Niño than La Niña years. That is, a higher frequency of typhoon landfalls is observed in those countries during El Niño years. Given a longer lifespan and a tendency for recurved tracks of tropical cyclones during El Niño years, this result is not unexpected. Conversely, typhoon landfalls become more common in the northern Philippines and the South China Sea during La Niña years, a result consistent with Chan (2000).

The Eastern and Central North Pacific

The average annual tropical cyclone number in the eastern and central North Pacific is 17, the second highest among the seven ocean basins (Neumann 1993). The standard deviation of the annual number of tropical cyclones is 4.1, the same as the western North Pacific. Given the smaller mean annual tropical cyclone counts in the eastern and central North Pacific, the same standard deviation in the two basins implies that there are larger interannual variations in tropical cyclone frequency in this basin. Unlike the western North Pacific, tropical cyclones in the eastern North Pacific do not occur in the cool season; the official hurricane season defined by the U.S. National Weather Service extends from May 15 to November 30 (OFCM 1999). A majority of the tropical cyclones form between the Mexican coast and Clipperton Island (~10°N, 110°W) and between 10°N and 15°N along the axis of the monsoon trough (figure 11.6).

In boreal summer, the strong southeast trades from the South Pacific cross the equator and turn into southwest currents in the eastern North Pacific. The

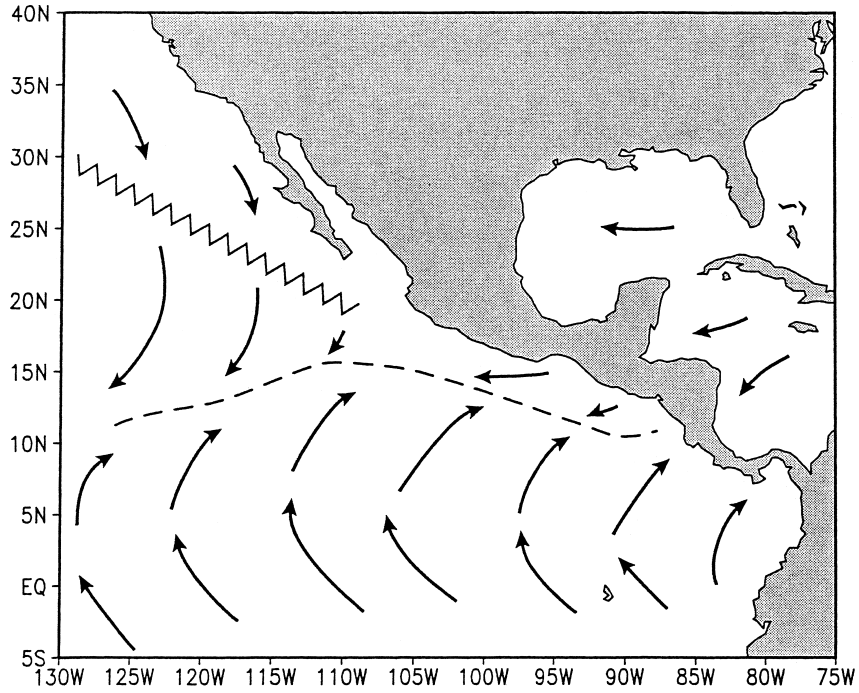

FIGURE 11.6 Schematic showing the long-term mean surface circulation in August in the eastern North Pacific. The monsoon trough axis is denoted by a broken line, and the ridge axis by a zigzag line. Wind directions are indicated by arrows.

low-latitude southwest monsoons meet the trade winds in the subtropics and form the monsoon trough where the sea-surface temperature is warm (≥ 28°C) and the vertical wind shear is weak. Tropical cyclones in the eastern North Pacific might also be triggered by tropical easterly waves from the North Atlantic (e.g., Rappaport et al. 1998). When tropical cyclones were active in the eastern North Pacific, they tended to be inactive over the North Atlantic and vice versa (Elsner and Kara 1999). Once formed, tropical cyclones generally track northwestward over the cooler water of the North Pacific and lose their strength gradually. Some tropical cyclones will occasionally curve northeastward and strike Mexico with lingering effects such as heavy rain and flooding in the southwest United States.

Whitney and Hobgood (1997) failed to find an ENSO impact on the overall tropical cyclone frequency in the eastern North Pacific. For instance, the average annual number of tropical cyclones (named storms) is 15.1 during El Niño but 15.0 for non–El Niño, based on records from 1963 to 1993. If only intense hurricanes (i.e., category three or above on the Saffir-Simpson hurri-

cane disaster potential scale) for the last 30 years are considered, however, the ratio of intense hurricanes during warm to cold years is about 1.7. Note that the intense hurricane comparison uses six warm and cold ENSO years described in the previous section on the western North Pacific. This result is consistent with that of Gray and Sheaffer (1991), who found that the number of intense hurricanes (i.e., wind speeds of at least 50 m s^{-1}) during El Niño years increases by a factor of two compared to that during La Niña years. It is not yet clear what physical mechanisms are responsible for a higher number of intense hurricanes during El Niño years. Collins and Mason (2000), however, pointed out the need to study the eastern North Pacific by subregions because environmental parameters affecting tropical cyclone activity are different east and west of 116°W.

Although the overall cyclone frequency over the eastern North Pacific did not change appreciably during two opposite extreme climatic events, the cyclone track and its longevity have changed. In analyzing tropical cyclone tracks for warmest and coldest ENSO events, Schroeder and Yu (1995) and Kimberlain (1999) noted a westward expansion of tropical cyclone tracks during warm events and eastward retreat during cold events. Interestingly, the genesis location also appears to be changed from warm to cold events. According to Irwin and Davis (1999), the mean longitude of tropical cyclone origin points during the storm season shifted 5.7º west in the negative SOI phase (El Niño) relative to the positive phase (La Niña). During the positive SOI phase, tropical cyclones are more likely to form near the Mexican coast. Kimberlain (1999) also suggested that tropical cyclone lifetimes in the eastern and central North Pacific are longer during El Niño years relative to La Niña years, and this difference is statistically significant (a p-value of 0.02).

The central North Pacific covers an area between the date line and 140ºW and north of the equator (figure 11.1). This domain coincides with the area of responsibility for the Central Pacific Hurricane Center, an entity of the U.S. National Weather Service Forecast Office in Honolulu, Hawaii. Tropical cyclone counts include storms that form within the domain of the central North Pacific as well as storms that form in the eastern North Pacific and subsequently propagate into the central North Pacific. In this regard, two types of tropical cyclones (i.e., propagated from the east and formed in situ) appear in the central North Pacific.

Time series of the annual number of tropical cyclone in the central North Pacific are displayed in figure 11.7. One notable feature is a tendency for a relative maximum of tropical cyclone occurrences during some of the El Niño years (e.g., 1972, 1982, and 1997). There is also an indication of decadal variations with fewer cyclones from 1966 to 1981 and more from 1982 to 1994 (Chu

and Clark 1999). Moreover, the Quasi-Biennial Oscillation is also evident, particularly in the late 1970s and early 1990s. Although this is a simple time series, it reflects a multitude of various climate forcings on tropical cyclone activity. The ENSO influences on tropical cyclone frequency in the central North Pacific are further corroborated by the strong correlation coefficient between the SOI and tropical cyclone counts. The Pearson correlation between these two variables from 1966 to 1997 is –0.53, which is significant at the 1% level after climatological persistence is taken into account. Based on general circulation model simulations forced with observed monthly sea-surface temperatures in the tropical Pacific Ocean, Wu and Lau (1992) found that tropical storms in the central North Pacific form more often during El Niño events. Even if the focus is restricted to a smaller region near Hawai'i, the difference in the annual mean number of tropical cyclones between the El Niño and non–El Niño years is still statistically significant at the 5% level based on a two-sample permutation test (Chu and Wang 1997). It is surmised that tropical cyclone frequency during La Niña years is reduced relative to El Niño years.

To illustrate the difference in large-scale environmental conditions conducive to tropical cyclone development between extreme climatic events, figure 11.8 shows the low-level vorticity field in July-September for the El Niño and La Niña composites. This is the peak tropical cyclone season in the central

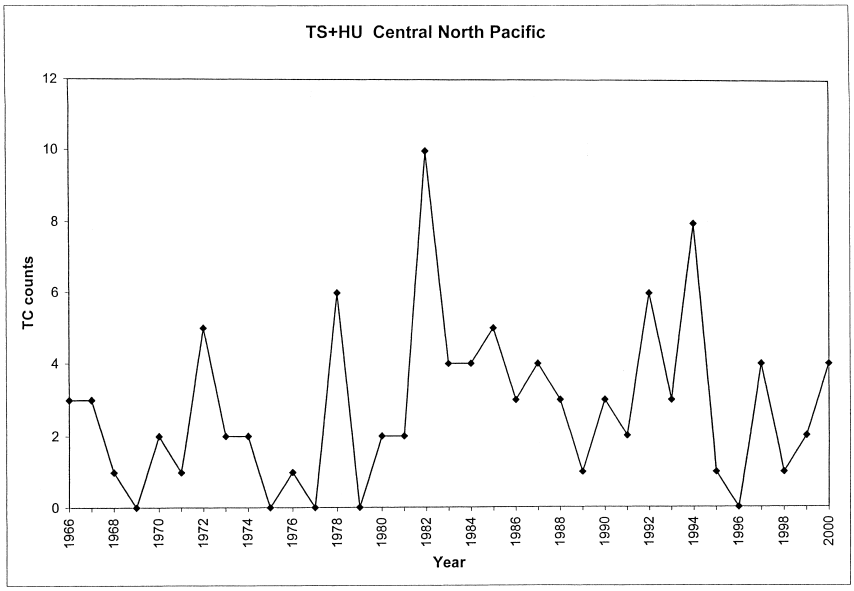

FIGURE 11.7 Time series of annual tropical cyclone numbers in the central North Pacific for the years 1966 through 2000. Only tropical storms and hurricanes are included.

North Pacific. The vorticity data at the 1,000 hPa level are obtained from the NCEP/NCAR Reanalysis Project (Kalnay et al. 1996). The band of cyclonic (positive) relative vorticity in the El Niño composite is two to three times greater in the broad region from 150°E to 165°W to the south of Hawai'i when compared to the La Niña composite. This increase in cyclonic vorticity is mainly attributed to the eastward extension of the monsoon trough during El Niño years (figure 11.4). When coupled with other favorable environmental conditions such as a decrease in vertical wind shear (not shown) and a possible enhancement in moist layer depth due to boundary layer moisture convergence by the spin-up process, this increase in low-level cyclonic vorticity accounts for more tropical cyclone formation in the central North Pacific.

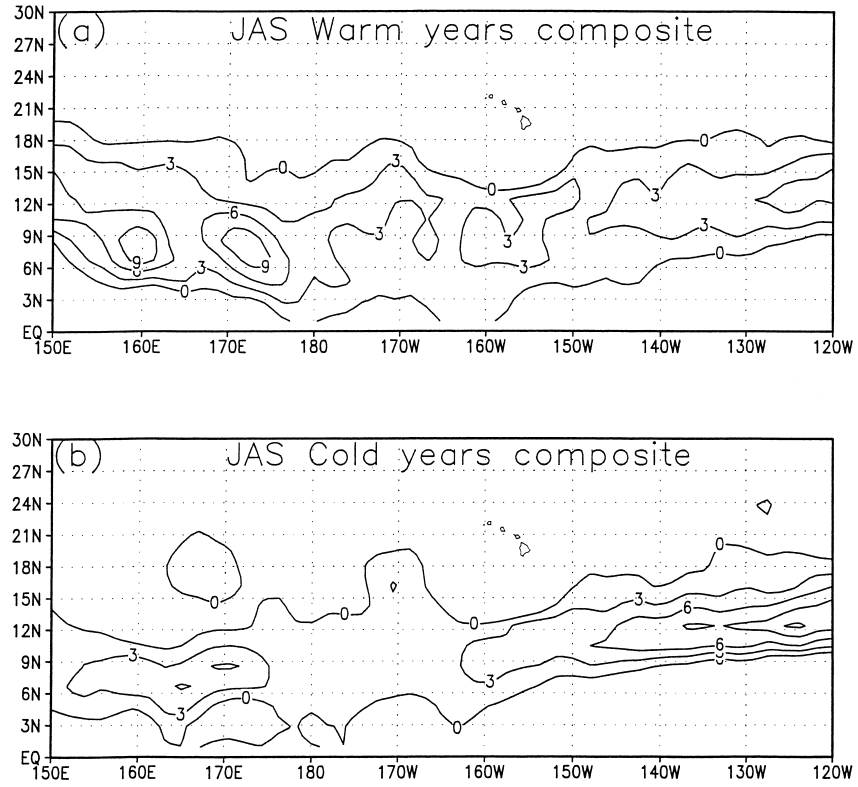

FIGURE 11.8 July through September (JAS) 1,000 hPa mean relative vorticity in the North Pacific for (*a*) El Niño (warm years) composite and (*b*) La Niña (cold years) composite. Units are 10^{-6} s^{-1} and the contour interval is 3. Only positive values are contoured. Years considered for the El Niño batch include 1972, 1982, 1986, 1987, 1991, and 1997. For the La Niña batch, only five cases (1970, 1973, 1975, 1988, and 1998) are considered, as data for 1999 are unavailable. Due to topographical influences on surface winds near Hawai'i, the vorticity field in the vicinity of the Hawaiian Islands is masked.

The westward shift in the genesis location of tropical cyclones in the eastern North Pacific during El Niño years (Irwin and Davis 1999) would tend to propagate tropical cyclones farther west into the central Pacific. In addition, the decrease in vertical shear over the tropical central North Pacific in El Niño years would reduce the unfavorable conditions for tropical cyclones and make it more likely for tropical cyclones to propagate into the central North Pacific. Tropical cyclone tracks near the Hawaiian Islands also show marked differences that are associated with interannual climate variations. For non–El Niño years, most tropical cyclones follow a westward or northwestward track, but they become more erratic during El Niño years (Chu and Wang 1997).

The South Pacific

Nicholls (1979) first noted a strong correlation between the sea level pressure in Darwin, Australia, and tropical cyclone days around the Australian region (105°E–165°E). During the period from 1958–1959 to 1982–1983, the linear correlation between the preseason sea level pressure (July to September) and the number of tropical cyclone days in the cyclone season (October to April) is –0.68, which is significant at the 5% level. Because the Darwin pressure is a major component of the SOI (note that the standard SOI is inversely related to Darwin pressure), this strong and negative correlation implies that a reduction in tropical cyclone days during the cyclone season near Australia is preceded by an anomalously high pressure in Darwin, or a warm event. Higher sea level pressures, cooling of ocean surfaces, and the sinking branch of the Pacific Walker circulation during El Niño years combine to produce unfavorable conditions for tropical cyclone formation near Australia. Nicholls (1985) further suggested that seasonal tropical cyclone activity in the Australian region can be predicted provided Darwin pressures are known a few months prior to the cyclone season. Nicholls, Landsea, and Gill (1998) found an artificial bias in the Australian region storms before 1983. After accounting for this bias, a strong tropical cyclone-ENSO association still remains (Nicholls, Landsea, and Gill 1998).

Hastings (1990) and Evans and Allan (1992) also noted an increased tropical cyclone frequency near the date line as well as reduced activity to the northeast of Australia during El Niño years (figure 11.1). Tropical cyclone tracks in the tropical southwestern Pacific (west of the date line) became more zonal during El Niño years. In contrast, tropical cyclones tracked close to the coast of Queensland, Australia, and persisted southward with enhanced risk for coastal crossings during La Niña years. Basher and Zheng (1995) performed a similar study investigating the spatial patterns of tropical cyclones in the southwestern Pacific in relation to the ENSO and regional sea-surface temperatures. They

suggested that the incidence of tropical cyclones in the Coral Sea (west of 170°E) is influenced by local sea-surface temperature and east of 170°E the dominant control is not local sea-surface temperature but the eastward extent of ENSO-dependent atmospheric conditions (i.e., the monsoon trough).

As described earlier, tropical cyclones in the western Pacific generally spawn in the vicinity of the monsoon trough. For the South Pacific, the eastern terminus of the trough is usually located near 174°E (figure 11.9). Figure 11.10a shows a surface streamline analysis on November 15, 1982, at the height of the very strong 1982–1983 El Niño event. At that time, a pair of elongated monsoon troughs that extended as far east as 140°W were noted, one in each hemisphere. The South Pacific trough was almost 60° of longitude (~6,600 km) east of its November mean position. Embedded between this pair of troughs were equatorial westerlies that extended conspicuously all the way from the western to the central and eastern Pacific; the westerlies were several thou-

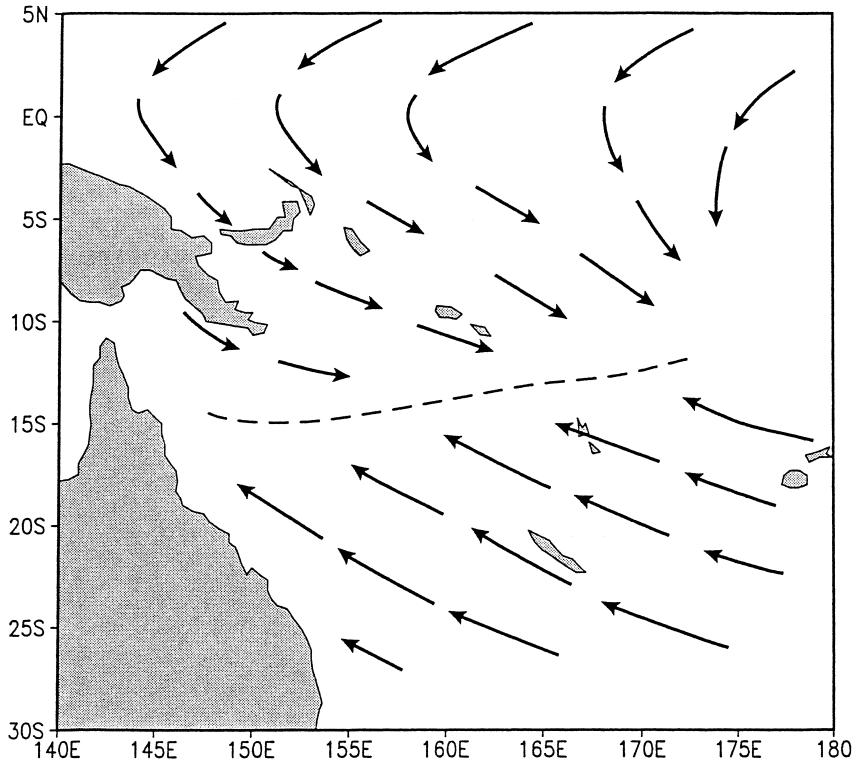

FIGURE 11.9 Schematic showing the long-term mean surface circulation in February in the southwestern Pacific. The monsoon trough axis is indicated by a broken line. Wind directions are indicated by arrows.

sand kilometers in extent. The double trough provided a favorable breeding ground for twin tropical cyclones on each side of the equator. The South Pacific cyclone formed near 8ºS, 165ºW and moved to the south of Penrhyn (figure 11.10a). The North Pacific counterpart, tropical storm Iwa, formed near 8°N, 167°W on November 18, 1982 (not shown). It then intensified to hurricane strength and inflicted major damages ($250 million) on Kauai, Hawai'i (Chu and Wang 1998). In March 1983, the South Pacific monsoon trough was still active and could be identified between 170ºE and 135ºW (figure 11.10b). Strong and persistent equatorial westerlies continued to move eastward, reaching beyond 110ºW by May 1983. These El Niño related conditions were unusual because the southeastern Pacific is generally dominated by steady easterly trade winds.

Equatorial westerly winds and easterly trade winds in the subtropics generate low-level cyclonic shear and cyclonic relative vorticity. In doing so, they create an environment along the monsoon trough that is favorable for tropical cyclone formation. Moreover, the anomalously warm ocean surface over the central and eastern Pacific during El Niño years fuels the overlying atmosphere with additional heat and moisture, decreasing atmospheric stability and increasing the likelihood of atmospheric convection. Taken together, these dynamic and thermodynamic factors are instrumental in maintaining and generating tropical cyclones. Anomalous conditions during an El Niño may cause tropical cyclones to occur in a region that is not generally regarded as a cyclone-prone area, for example, the Hawaiian Islands in the North Pacific or French Polynesia in the South Pacific.

In accordance with the displacement of the monsoon trough and equatorial westerlies during the 1982–1983 El Niño, the genesis locations of tropical cyclones moved eastward with time (figure 11.11). Climatologically, this area is marked by strong vertical wind shears as the prevailing surface northeasterlies are overlain by southerlies in the upper troposphere. But from December 1982 through May 1983, 11 tropical cyclones were named in the southeastern Pacific. Three unnamed tropical depressions also developed in the eastern end of the South Pacific. Tropical cyclones east of 160ºW are rare. During the 1982–1983 El Niño, however, six hurricanes struck French Polynesia (Sadler 1983). The recurvature of storms such as Veena and William is conspicuous.

In analyzing a 40-year sample (1939–1940 to 1978–1979) of tropical cyclone genesis locations in the South Pacific, Revell and Goulter (1986) noted eastward and equatorward displacements of the origin points during El Niño years as compared to non–El Niño years, a result subsequently confirmed by Basher and Zheng (1995). For instance, the climatological median location of genesis point is 14ºS, 170ºE near Vanuatu (Revell and Goulter 1986). During 1982–1983, the

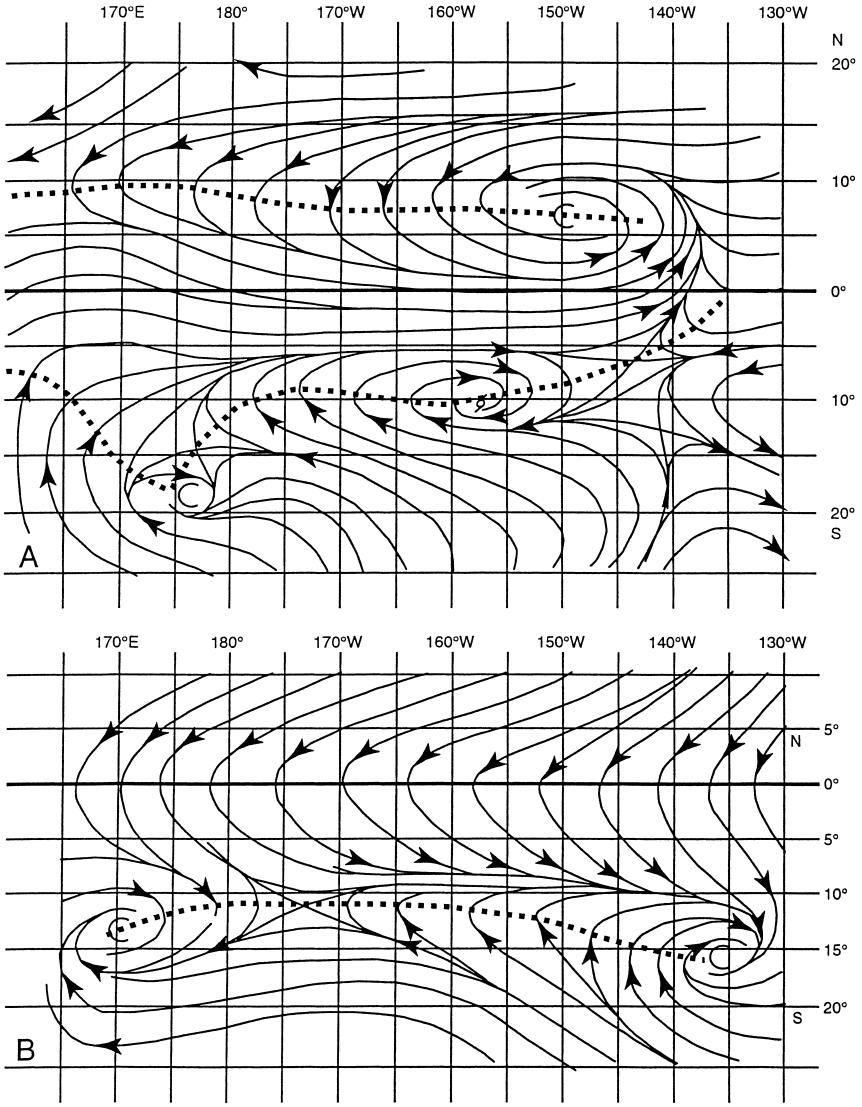

FIGURE 11.10 Surface streamline analyses for (*A*) November 15, 1982, and (*B*) March 21, 1983. The trough lines are indicated by dots. Note that in (*A*) the equatorial westerlies in the central Pacific are embedded between the double trough, one in each hemisphere, and that the tropical depression near Penryhn in the South Pacific (~158°W) is indicated. In (*B*), westerlies lie between the trough (dotted line) and the equator. Note the trough extends as far east as 135°W (adapted from Sadler, 1983, with permission).

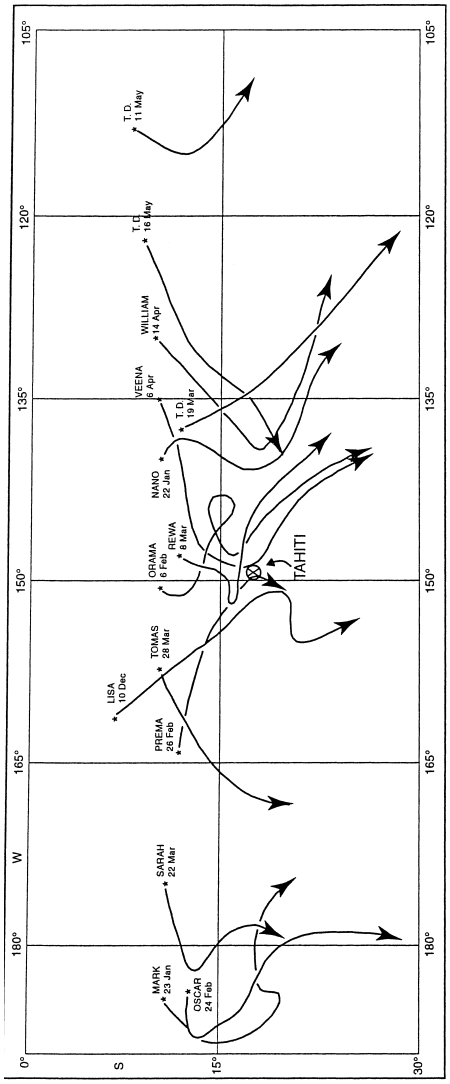

FIGURE 11.11 Tracks of southeastern Pacific tropical cyclones from December 1982 to May 1983. Asterisk indicates origin points of tropical depression (adapted from Sadler 1983, with permission).

median origin point shifted northeastward to 11ºS, 162ºW, a remarkable eastward displacement by almost 28º longitude (~3,000 km) from its climatological median location. The meridional displacement of the median genesis location during the 1982–1983 El Niño event is 3º latitude equatorward from the climatological position. These dramatic displacements of origin points are intimately related to the migration of the South Pacific monsoon trough and the South Pacific convergence zone as suggested by Revell and Goulter (1986).

Figure 11.12 illustrates tropical cyclone origins and tracks for another very strong 1997–1998 warm ENSO event, as downloaded from the Australian Severe Weather Web site (http://australiansevereweather.simplenet.com). During 1997 and 1998, the median location of genesis points for all named storms in the South Pacific was 12.2ºS, 170.2ºW, again a 20º longitudinal shift eastward from the climatological median position. During this warm event, tropical cyclones were more frequent in the South Pacific and they also formed in late season, as typified by Alan and Bart in late April 1998. This result is similar to what happened in 1983 (figure 11.11). The Cook Islands and French Polynesia were constantly under the threat of tropical cyclone strikes. There was also an unusual westward storm track between 10°S and 15°S to the west of 170°E (figure 11.12), a feature that is not uncommon during warm ENSO years (Evans and Allan 1992).

For the sake of comparison, it is also instructive to examine tropical cyclone activity in the South Pacific during the recent 1998–1999 La Niña years. From July 1998 to June 1999, only three cyclones with at least tropical storm strength were observed in the South Pacific to the east of the date line. In contrast, 11 cyclones occurred in the same region during the 1997–1998 El Niño episode (figure 11.12).

The North Atlantic

The mean annual number of tropical cyclones in the north Atlantic is 10, a smaller number in comparison to that found in the northwestern or northeastern Pacific. Most hurricanes in this basin occur between June and November, with 83% of the total annual numbers occurring in August, September, and October. Peak hurricane activity occurs in September with a 90% chance of at least one hurricane (Elsner and Kara 1999). In a series of papers, Gray (1984), Gray and Sheaffer (1991), and Gray et al. (1993), and Knaff (1997) found that interannual variations in the seasonal activity of Atlantic hurricanes can be correlated with several variables because of their effects on vertical wind shear in the troposphere. These variables include, but are not limited to, ENSO, Atlantic Basin sea level pressure, west Sahel monsoon rainfall, and the Quasi-

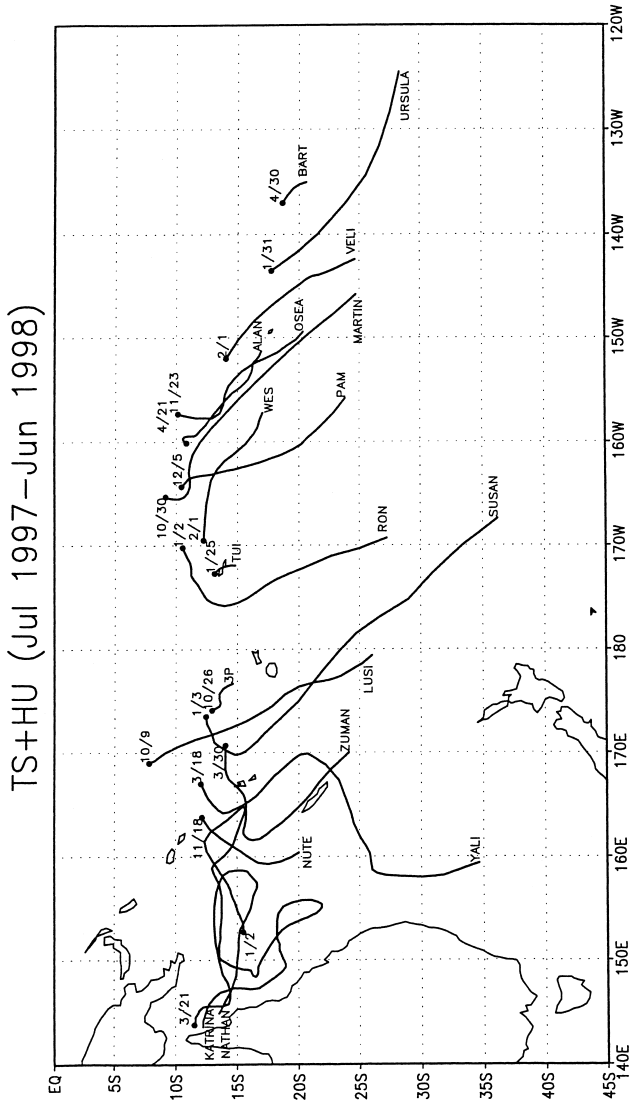

FIGURE 11.12 Tracks of South Pacific tropical cyclones from July 1997 to June 1998. Tropical depressions are omitted. Origin points are denoted by dots, and the month and date for each tropical cyclone are indicated by numbers. Termination points of track are marked by the name of cyclones.

Biennial Oscillation of stratospheric wind. Shapiro (1987) was able to show a statistical relationship between vertical wind shear and an El Niño index. Subsequently, Goldenberg and Shapiro (1996) provided evidence that changes in vertical wind shear are the most important environmental factor modulating Atlantic hurricane activity on interannual time scales.

During El Niño, the warm pool of sea water and major tropical convection shift eastward to the eastern Pacific. ENSO alters Atlantic hurricane activity through shifts in the location of large-scale convection. The enhanced upper-level divergent outflows from deep cumulus convection cause upper tropospheric zonal winds over the Caribbean and tropical Atlantic to become more westerly. ENSO's influence on lower-tropospheric easterly winds over the tropical Atlantic is small so vertical wind shear over the tropical Atlantic and Caribbean region is enhanced during the El Niño hurricane season (Gray and Sheaffer 1991). Consequently, the number of hurricanes and hurricane days are reduced during El Niño years (Landsea et al. 1999). In addition to the wind-shear mechanism, the western North Atlantic is marked by subsidence during warm ENSO phases, another factor unfavorable for hurricane development (figure 11.2).

The ENSO phenomenon also affects the U.S. hurricane landfalls (Gray 1984). Assuming that the occurrence of U.S. hurricanes follows a Poisson distribution, Bove et al. (1998) showed that the probability of a landfalling hurricane is reduced during El Niño events but increased during La Niña events. For instance, the probability of observing two or more landfalling hurricanes during an El Niño is 28%, in contrast to 66% during La Niña (figure 11.13). Thus, the La Niña phase has a profound impact on U.S. hurricane landfalls. Landfall probability for the neutral phase lies between these two extremes. In terms of economic losses, the average damage per storm is $800 million during El Niño years but doubles to $1.6 billion during La Niña years (Pielke and Landsea 1999). More interestingly, there is a 20 to 1 ratio in median damage per year during two extreme climatic events: $3.3 billion in La Niña years versus $152 million in El Niño years.

Elsner and Kara (1999) further partitioned Atlantic hurricanes into tropical-only and baroclinically enhanced groups and noted that the ENSO influence occurs for tropical-only systems. In addition, Elsner and Kara (1999) found a difference in genesis locations throughout the six-month hurricane season for two contrasting ENSO phases (figure 11.14). During El Niño, most tropical cyclones formed over the Gulf of Mexico in early season (June–July), and moved away from the continent to the western North Atlantic in mid-season (August–September) and late season (October–November). The mean latitu-

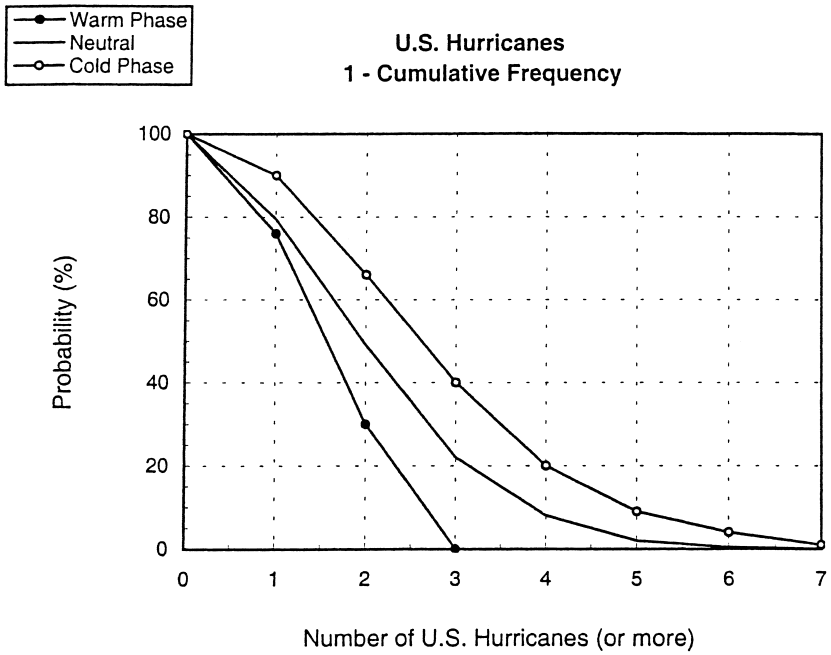

FIGURE 11.13 Inverse cumulative probability distributions for U.S. hurricane landfalls over the period from 1900 to 1997. Solid circle is for the warm ENSO phase, open circle is for the cold ENSO phase, and no circle is for the neutral condition (after Bove et al. 1998).

dinal location of genesis point is 23.7°N in early season, 23.2°N in mid-season, and 24.4°N in late season during El Niño. In contrast, during La Niña, the origin points of tropical cyclones are found off the southeast U.S. coast in early season, moving toward the Gulf of Mexico in mid-season, and shifting equatorward over the Caribbean Sea in late season. On average, the position of tropical cyclone formation point is found in lower latitudes during La Niña years when compared to El Niño years.

During extreme climatic events, a shift in the mean longitudinal location of tropical cyclone origin points is even more pronounced than that for the mean latitudinal location. For instance, the mean longitude is 88.9°W in early season, 62.8°W in mid-season, and 72.3°W in late season during El Niño. There is also a considerable west-east movement of the mean origin points throughout the hurricane season during La Niña years, from the Gulf of Mexico in early season (82°W), to the western North Atlantic in mid-season (64.9°W), and to the southwestern North Atlantic in late season (72.3°W). In analyzing tropical cyclone tracks during the course of El Niño, Gray and Sheaffer (1991) noted fewer hurricanes crossing through the Caribbean Basin in a

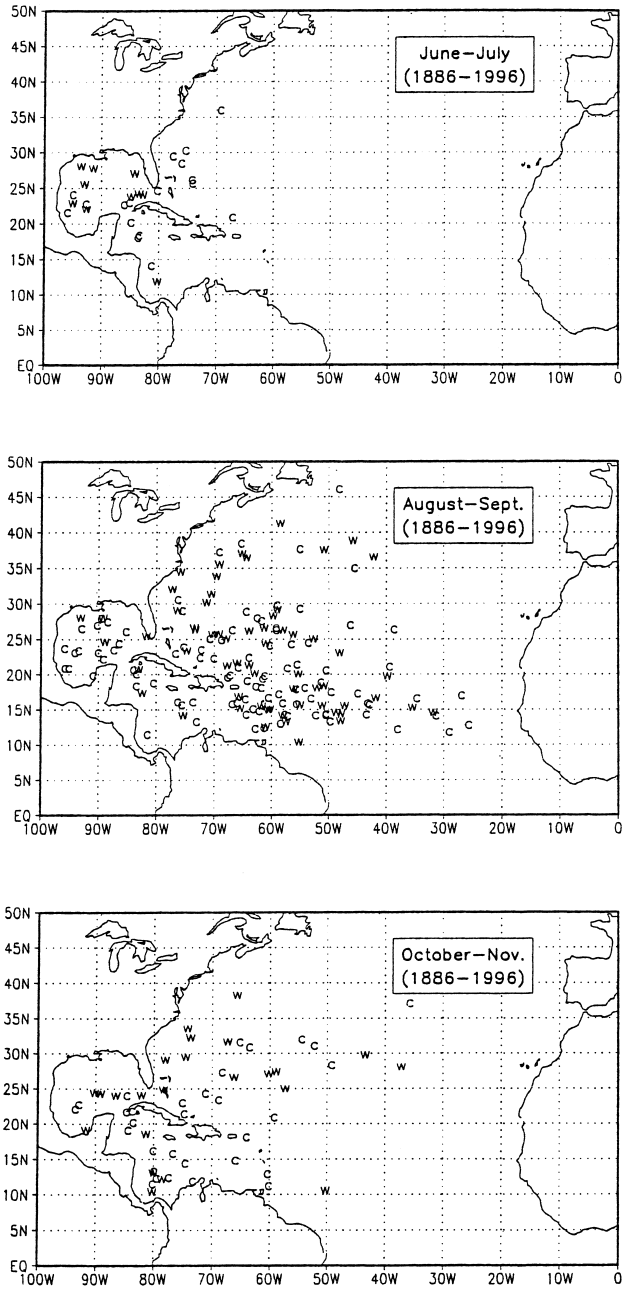

FIGURE 11.14 Origin points of North Atlantic hurricanes by season during warm (w) and cold (c) ENSO phases for the period 1886 to 1996 (from Elsner and Kara, 1999; reproduced with permission from Oxford University Press).

westward track during El Niño years compared to non–El Niño years. During the La Niña batch, the mean intensity, as measured by the average of the strongest winds for all named storms for a season, is only a bit stronger (6%) than the El Niño batch (Landsea et al. 1999).

Summary

This chapter has described the El Niño–Southern Oscillation (ENSO) phenomenon, which is the most dominant mode in year-to-year climate variations in the tropics, and its impact on tropical cyclone activity. It has been known for many years that on seasonal time scales tropical cyclone formation and development are intimately regulated by large-scale dynamic and thermodynamic environmental conditions (Gray 1977). An ENSO event alters large-scale environmental conditions and influences probability distributions that describe tropical cyclone attributes such as genesis location, frequency, track, lifespan, landfall, and intensity.

For the western North Pacific, the warm phase of ENSO shifts the monsoon trough to the east and reduces vertical wind shear. Low-level cyclonic vorticity associated with the monsoon trough nearly triples in the eastern portion during the warm phase. These changes are accompanied by a notable increase in tropical cyclone genesis and frequency in the eastern portion of the basin (150°E to the date line) (table 11.1). During the cold phase, tropical cyclone genesis locations at peak season stay at higher latitudes over the western extreme of the North Pacific. Tropical cyclone life spans are longer during the warm phase as most tropical cyclones form over lower latitude oceans and away from the large land masses. Tropical cyclones track mainly westward during La Niña years but they tend to recurve during El Niño years. As a result, typhoon impacts in Japan, South Korea, Taiwan, and China are more pronounced in El Niño than La Niña years.

The influence of two contrasting ENSO phases on the overall frequency of the eastern North Pacific hurricanes appears to be minimal (table 11.1), although more intense hurricanes are observed during the warm phase than in the cold one. Tropical cyclone genesis locations also shift westward and life spans are longer during El Niño years as opposed to La Niña years. Besides the monsoon trough (in-situ influence), tropical cyclone genesis in the eastern North Pacific is modulated by external forcings such as tropical easterly waves from the Caribbean.

The central North Pacific experiences an increased occurrence of tropical cyclones during the warm phase, and this increase is due to the eastward excur-

TABLE 11.1 ENSO and Tropical Cyclone Activity in the Pacific and Atlantic Oceans

Basin	Frequency	Genesis location	Intensity	Track	Life span
Northwestern Pacific	No significant changes in the developing year, but is reduced in the following year	Farther east and south	Unknown	More likely to recurve	Longer
Northeastern Pacific	Overall frequency unchanged	Farther west	More intense hurricanes	Westward expansion	Longer
Central North Pacific (180°W–140°W)	More storms	More likely to form in the western part	Unknown	More erratic	Unknown
Southwestern Pacific (west of dateline)	Fewer storms	Farther north	Unknown	Likely to track westward in the tropics	Unknown
Southeastern Pacific	More storms	Farther east and north	Unknown	unknown	Unknown
North Atlantic	Fewer storms	Farther north in mid- and late seasons	Slightly weaker	Fewer storms cross the lower Caribbean	Unknown

Note: Opposite changes are implied for La Niña.

sion of the monsoon trough from the western North Pacific and the combined effects of the weakening of the vertical wind shear as well as the westward shift of the genesis locations from the eastern North Pacific (table 11.1).

As in the western North Pacific, tropical cyclone frequency and genesis locations in the South Pacific undergo substantial changes during extreme ENSO events. Although most tropical cyclones form in the Coral Sea during non–El Niño years, they originate mainly to the east of the date line during the warm phase (table 11.1). Islands that are normally free from tropical cyclone

risks, such as French Polynesia, are threatened more often by tropical cyclones during strong, warm ENSO events.

In the North Atlantic, El Niño years are associated with fewer hurricanes and major hurricanes, fewer hurricane days and a lower probability of U.S. hurricane landfalls (table 11.1). During the cold phase the U.S. coast is faced with a higher risk of hurricane landfalls. The tropical cyclone genesis locations shift equatorward as the hurricane season progresses; thus the Caribbean Sea becomes more vulnerable to tropical cyclone risks in late season. Hurricanes crossing the lower Caribbean Basin also become more prevalent during non–El Niño years.

Acknowledgments

I would like to express my thanks to Maria Rakotondrafa for performing data and graphic analyses and Di Henderson for editing. Constructive review comments by Chris Landsea, Rick Murnane, Tom Schroeder, and an anonymous reviewer led to significant improvement in the presentation of this chapter.

References

Barnston, A. G., M. Chelliah, and S. B. Goldenberg. 1997. Documentation of a highly ENSO-related SST region in the equatorial Pacific. *Atmosphere-Ocean* 35:367–83.

Basher, R. E., and X. Zheng. 1995. Tropical cyclones in the southwest Pacific: Spatial patterns and relationships to Southern Oscillation and sea surface temperature. *Journal of Climate* 8:1249–60.

Battisti, D. S., and A. C. Hirst. 1989. Interannual variability in a tropical atmosphere-ocean model: Influence of basic state, ocean geometry and non-linearity. *Journal of Atmospheric Sciences* 46:1687–712.

Bjerknes, J. 1969. Atmospheric teleconnections from the tropical Pacific. *Monthly Weather Review* 97:163–72.

Bove, M. C., J. B. Elsner, C. W. Landsea, X. Niu, and J. J. O'Brien. 1998. Effect of El Niño on U.S. landfalling hurricanes, revisited. *Bulletin of the American Meteorological Society* 76:2477–82.

Cane, M. A., and S. E. Zebiak. 1985. A theory for El Niño and the Southern Oscillation. *Science* 228:1085–87.

Chan, J. C. L. 1985. Tropical cyclone activity in the northwest Pacific in relation to the El Niño/Southern Oscillation phenomenon. *Monthly Weather Review* 113: 599–606.

Chan, J. C. L. 2000. Tropical cyclone activity over the western North Pacific associated with El Niño and La Niña events. *Journal of Climate* 13:2960–72.

Chen, T.-C., S.-P. Weng, N. Yamazaki, and S. Kiehne. 1998. Interannual variation in the tropical cyclone formation over the western North Pacific. *Monthly Weather Review* 126:1080–90.

Chu, P.-S., and J. D. Clark. 1999. Decadal variations of tropical cyclone activity over the central North Pacific. *Bulletin of the American Meteorological Society* 80:1875–81.

Chu, P.-S., J. Frederick, and A. J. Nash. 1991. Exploratory analysis of surface winds in the equatorial western Pacific and El Niño. *Journal of Climate* 4:1087–102.

Chu, P.-S., and R. W. Katz. 1985. Modeling and forecasting the Southern Oscillation: A time-domain approach. *Monthly Weather Review* 113:1876–88.

Chu, P.-S., and R. W. Katz. 1989. Spectral estimation from time series models with relevance to the Southern Oscillation. *Journal of Climate* 2:86–90.

Chu, P.-S., and J. Wang. 1997. Tropical cyclone occurrences in the vicinity of Hawaii: Are the differences between El Niño and non-El Niño years significant? *Journal of Climate* 10:2683–89.

Chu, P.-S., and J. Wang. 1998. Modeling return periods of tropical cyclone intensities in the vicinity of Hawaii. *Journal of Applied Meteorology* 37:951–60.

Clark, J. D., and P.-S. Chu. 2002. Interannual variation of tropical cyclone activity over the central North Pacific. *Journal of the Meteorological Society of Japan* 80:403–18.

Collins, J. M., and I. M. Mason. 2000. Local environmental conditions related to seasonal tropical cyclone activity in the Northeast Pacific basin. *Geophysical Research Letters* 27:3881–84.

Deser, C., and J. M. Wallace. 1990. Large-scale atmospheric circulation features of warm and cold episodes in the tropical Pacific. *Journal of Climate* 3:1254–81.

Dong, K. 1988. El Niño and tropical cyclone frequency in the Australian region and the northwest Pacific. *Australian Meteorological Magazine* 36:219–25.

Elsner, J. B., and A. B. Kara. 1999. *Hurricanes of the North Atlantic: Climate and society*. New York: Oxford University Press.

Evans, J. L., and R. J. Allan. 1992. El Niño/Southern Oscillation modification to the structure of the monsoon and tropical activity in the Australian region. *International Journal of Climatology* 12:611–23.

Frank, W. M. 1987. Tropical cyclone formation. In *A Global view of tropical cyclones*, edited by R. L. Elsberry, W. M. Frank, G. J. Holland, J. D. Jarrell, and R. L. Southern, 53–90. Chicago: University of Chicago Press.

Goldenberg, S. B., and L. J. Shapiro. 1996. Physical mechanisms for the association of El Niño and West Africa rainfall with Atlantic major hurricanes. *Journal of Climate* 9:1169–87.

Gray, W. M. 1968. Global view of the origin of tropical disturbances and storms. *Monthly Weather Review* 96:55–73.

Gray, W. M. 1977. Tropical cyclone genesis in the western North Pacific. *Journal of the Meteorological Society of Japan* 55:465–82.

Gray, W. M. 1984. Atlantic seasonal hurricane frequency. Part I: El Niño and 30 mb Quasi-Biennial Oscillation influences. *Monthly Weather Review* 112:1649–68.

Gray, W. M., C. W. Landsea, P. W. Mielke, Jr., and K. J. Berry. 1993. Predicting Atlantic basin seasonal tropical cyclone activity by 1 August. *Weather and Forecasting* 8:73–86.

Gray, W. M., and J. D. Sheaffer. 1991. El Niño and QBO influences on tropical cyclone activity. In *Teleconnections linking worldwide climate anomalies*, edited by M. H. Glantz, R. W. Katz, and N. Nicholls, 257–84. New York: Cambridge University Press.

Hastings, P. A. 1990. Southern Oscillation influences on tropical cyclone activity in the Australian/South-west Pacific region. *International Journal of Climatology* 10:291–98.

Irwin, R. P., and R. E. Davis. 1999. The relationship between the Southern Oscillation Index and tropical cyclone tracks in the eastern North Pacific. *Geophysical Research Letters* 20:2251–54.

Jin, F.-F. 1997. An equatorial ocean recharge paradigm for ENSO. Part I: Conceptual model. *Journal of Atmospheric Sciences* 54:811–29.

Jury, M. 1993. A preliminary study of climatological associations and characteristics of tropical cyclones in the southwest Indian Ocean. *Meteorological + Atmospheric Physics* 51:101–15.

Kalnay, E., et al. 1996. The NCEP/NCAR 40-year reanalysis project. *Bulletin of the American Meteorological Society* 77:437–71.

Kimberlain, T. B. 1999. The effects of ENSO on North Pacific and North Atlantic tropical cyclone activity. In *Preprints of the 23rd Conference on Hurricanes and Tropical Meteorology*, 250–53. Boston: American Meteorological Society.

Kimberlain, T. B. 2000. Long-term trends in North Pacific tropical cyclone activity. In *Preprints of the 24th Conference on Hurricanes and Tropical Meteorology*, 472–73. Boston: American Meteorological Society.

Kirtman, B., ed. 2001. *Experimental Long-Lead Forecast Bulletin* 10, no. 1 (available at: http://www.iges.org/ellfb).

Knaff, J. A. 1997. Implications of summertime sea level pressure anomalies in the tropical Atlantic region. *Journal of Climate* 10:789–804.

Knaff, J. A., and C. W. Landsea. 1997. An El Niño–Southern Oscillation Climatology and Persistence (CLIPER) forecasting scheme. *Weather and Forecasting* 12:633–52.

Lander, M. A. 1994. An exploratory analysis of the relationship between tropical storm formation in the western North Pacific and ENSO. *Monthly Weather Review* 122:636–51.

Lander, M. A. 1996. Specific tropical cyclone track types and unusual tropical cyclone motions associated with a reverse-oriented monsoon trough in the western North Pacific. *Weather and Forecasting* 11:170–86.

Landsea, C. W. 2000. El Niño–Southern Oscillation and the seasonal predictability of tropical cyclones. In *El Niño: Multiscale variability and global and regional impacts*, edited by H. F. Díaz and V. Markgraf, 149–81. Cambridge: Cambridge University Press.

Landsea, C. W., and J. A. Knaff. 2000. How much skill was there in forecasting the very strong 1997–98 El Niño? *Bulletin of the American Meteorological Society* 81:2107–19.

Landsea, C. W., R. A. Pielke, Jr., A. M. Mestas-Nuñez, and J. A. Knaff. 1999. Atlantic Basin hurricanes: Indices of climatic changes. *Climatic Change* 42:89–129.

Lee, H.-K., P.-S. Chu, C.-H. Sui, and K.-M. Lau. 1998. On the annual cycle of latent heat fluxes over the equatorial Pacific using TAO buoy observations. *Journal of the Meteorological Society of Japan* 76:909–23.

Lukas, R., S. P. Hayes, and K. Wyrtki. 1984. Equatorial sea-level response during the 1982–83 El Niño. *Journal of Geophysical Reserach* C 6:10425–30.

Madden, R. A., and P. R. Julian. 1971. Detection of a 40–50 day oscillation in the zonal wind in the tropical Pacific. *Journal of Atmospheric Sciences* 28:702–8.

McBride, J. L. 1995. Tropical cyclone formation. In *Global perspectives on tropical cyclones*, edited by R. L. Elsberry, 63–105. Report No. TCP-38. Geneva: World Meteorological Organization.

McCreary, J., Jr. 1983. A model of tropical ocean-atmosphere interaction. *Monthly Weather Review* 111:370–87.

Neumann, C. J. 1977. A critical look at statistical hurricane prediction models. In *Preprints of the 11th Conference on Hurricanes and Tropical Meteorology*, 375–80. Boston: American Meteorological Society.

Neumann, C. J. 1993. Global overview. In *Global guide to tropical cyclone forecasting*, edited by G. J. Holland, 1.1–1.56. Technical Document WMO/TC-No. 560, Report No. TCP-31. Geneva: World Meteorological Organization.

Nicholls, N. 1979. A possible method for predicting seasonal tropical cyclone activity in the Australian region. *Monthly Weather Review* 107:1221–24.

Nicholls, N. 1985. Predictability of interannual variations of Australian seasonal tropical cyclone activity. *Monthly Weather Review* 113:1144–49.

Nicholls, N. 1992. Recent performance of a method for forecasting Australian seasonal tropical cyclone activity. *Australian Meteorological Magazine* 21:105–10.

Nicholls, N., C. W. Landsea, and J. Gill. 1998. Recent trends in Australian region tropical cyclone activity. *Meteorological + Atmospheric Physics* 65:197–205.

Office of the Federal Coordinator for Meteorological Services and Supporting Research (OFCM). 1999. *National Hurricane Operations Plan (NHOP)*. FCM-P12–1999. Washington, D.C.: National Oceanic and Atmospheric Administration.

Pielke, R. A., Jr., and C. W. Landsea. 1999. La Niña, El Niño, and Atlantic hurricane damages in the United States. *Bulletin of the American Meteorological Society* 80:2027–33.

Rappaport, E. N., L. A. Avila, M. B. Lawrence, B. M. Mayfield, and R. J. Pasch. 1998. Eastern North Pacific hurricane season of 1995. *Monthly Weather Review* 126:1152–62.

Rasmusson, E. M., and T. H. Carpenter. 1982. Variations in tropical sea surface temperature and surface wind fields associated with the Southern Oscillation/El Niño. *Monthly Weather Review* 110:354–84.

Revell, C. G., and S. W. Goulter. 1986. South Pacific tropical cyclones and the Southern Oscillation. *Monthly Weather Review* 114:1138–45.

Sadler, J. 1967. *The tropical upper tropospheric trough as a secondary source of typhoons and a primary source of tradewind disturbances*. Report No. HIG-67-12.Honolulu: Department of Meteorology, University of Hawai'i.

Sadler, J. 1983. Tropical Pacific atmospheric anomalies during 1982–83. In *Proceedings of the 1982/83 El Niño/Southern Oscillation Workshop*, 1–10. Miami: National Oceanic and Atmospheric Administration and Atlantic Oceanographic and Meteorological Laboratory.

Saunders, M. A., R. E. Chandler, C. J. Merchant, and F. P. Roberts. 2000. Atlantic hurricanes and northwest Pacific typhoons: ENSO spatial impacts on occurrence and landfall. *Geophysical Research Letters* 27:1147–50.

Schopf, P. S., and M. J. Suarez. 1988. Vacillations in a coupled ocean-atmosphere model. *Journal of Atmospheric Sciences* 45:549–66.

Schroeder, T. A., and Z.-P. Yu. 1995. Interannual variability of central Pacific tropical cyclones. In *Preprints of the 21st Conference on Hurricanes and Tropical Meteorology*, 437–39. Boston: American Meteorological Society.

Shapiro, L. J. 1987. Month-to-month variability of the Atlantic tropical circulation and its relationship to tropical storm formation. *Monthly Weather Review* 115:2598–14.

Trenberth, K. E. 1976. Spatial and temporal variations of the Southern Oscillation. *Quarterly Journal of the Royal Meteorological Society* 102:639–53.

Trenberth, K. E. 1997. The definition of El Niño. *Bulletin of the American Meteorological Society* 78:2771–77.

Wang, B., and J. C. L. Chan. 2002. How strong ENSO affect tropical storm activity over the western North Pacific. *Journal of Climate* 15:1643–58.

Whitney, L. D., and J. Hobgood. 1997. The relationship between sea surface temperatures and maximum intensities of tropical cyclones in the eastern North Pacific Ocean. *Journal of Climate* 10:2921–30.

Wu, G., and N.-C. Lau. 1992. A GCM simulation of the relationship between tropical storm formation and ENSO. *Monthly Weather Review* 120:958–77.

Wyrtki, K. 1975. El Niño: The dynamic response of the equatorial Pacific Ocean to atmospheric forcing. *Journal of Physical Oceanography* 5:572–84.

Wyrtki, K. 1982. The Southern Oscillation, ocean-atmosphere interaction and El Niño. *Marine Technical Society Journal* 16:3–10.

Wyrtki, K. 1985. Water displacements in the Pacific and the genesis of El Niño cycles. *Journal of Geophysical Research* 90:7129–32.

Zebiak, S. E., and M. A. Cane. 1987. A model El Niño–Southern Oscillation. *Monthly Weather Review* 115:2262–78.